Science & Technology Development Journal 2025, 28(3):3817-3822

Open Access Full Text Article

Research Article

Synergistic Au/Ag-based SERS platform for sensitive detection of malachite green

Nhu Hoa Thi Tran[1,2,*], Bao Khanh Hoang[1,2], Nguyen Tran Truc Phuong [3], Do Quynh Nhu Nguyen[1,2], Bao Tran Nguyen[1,2], Hong Tho Le[2,4], T.T. Van Tran[1,2], Hieu Van Le [1,2,5], Dung Van Hoang[2,5]

ABSTRACT

Introduction: Malachite green (MG), a toxic and carcinogenic triphenylmethane dye widely used in aquaculture, has been restricted in many regions due to health and environmental concerns; however, it remains prevalent in some areas because of its low cost and strong efficacy. Although various methods have been employed to detect MG, surface-enhanced Raman scattering (SERS) offers rapid, high-sensitivity analysis by leveraging noble metal nanostructures and their localized surface plasmon resonance.

Methods: The SERS method for detecting MG leverages the localized surface plasmon resonance (LSPR) of gold (Au) and silver (Ag): these noble metal nanoparticles (NPs) create ``hot spots'' that concentrate electromagnetic energy. When MG molecules are adsorbed onto the Au/Ag surface, their Raman scattering signal is significantly amplified, allowing for detection at low concentrations. By employing a multilayer structure containing Au and Ag, the LSPR effect is optimized, resulting in a higher detection efficiency compared to single-layer metal substrates.

Results: Characterization via UV-Vis spectroscopy and XRD confirmed that Au and Ag NPs exhibit distinct plasmon absorption peaks (407 and 526 nm, respectively) and the (111) lattice plane at $2\theta = 38.2°$. HR-TEM and FE-SEM revealed that the Au NPs are spherical (30.46-nm diameter), and the Ag NPs measure 20 nm in diameter. SERS experiments with MG indicated that the P/Au/Ag substrate provides the highest enhancement, detecting MG down to 10^{-9} M.

Conclusions: The P/Au/Ag substrate for SERS-based MG detection was successfully fabricated and characterized, achieving a detection limit of 10^{-9}M. The robust multilayer structure, boosted by the synergy between Au and Ag, holds significant potential for trace-level detection of various contaminants in environmental monitoring and food safety.

Key words: Malachite green, SERS, Au/Ag, multilayers, handheld

[1]*Faculty of Materials Science and Technology, University of Science, Ho Chi Minh City, Vietnam*

[2]*Vietnam National University, Ho Chi Minh City, Vietnam*

[3]*NTT Hi-Tech Institute, Nguyen Tat Thanh University, Ward 13, District 04, Ho Chi Minh City, Viet Nam*

[4]*Center for Innovative Materials and Architectures (INOMAR), HoChiMinh City, Vietnam*

[5]*Laboratory of Advanced Materials, University of Science, Ho Chi Minh City, Vietnam*

Correspondence

Nhu Hoa Thi Tran, Faculty of Materials Science and Technology, University of Science, Ho Chi Minh City, Vietnam

Vietnam National University, Ho Chi Minh City, Vietnam

Email: ttnhoa@hcmus.edu.vn

History

- Received: 02-03-2025
- Revised: 15-06-2025
- Accepted: 21-06-2025
- Published Online: 18-09-2025

DOI :

https://doi.org/10.32508/stdj.v28i3.4432

INTRODUCTION

Malachite green (MG), a triphenylmethane dye, is commonly used as an ectoparasiticide, fungicide, and antiseptic in aquaculture because it can prevent fungal and parasite infections in fish[1]. The use of MG in aquaculture has garnered significant attention due to its established toxicity and carcinogenic properties, resulting in its classification as a Class II health hazard[2]. MG is deemed safe when its concentration falls within the minimum required performance limit (MRPL), 1–2 μg/kg[3]. Some reports have indicated that MG poses significant risks to human health due to its severely poisonous nature, along with its potential to cause cancer, birth defects, and genetic mutations. Furthermore, trace amounts of MG in aquaculture water can lead to substantial water contamination. As a consequence, several nations and regions have implemented regulations or, in some cases, completely prohibited its use in aquaculture; yet, its affordability and effectiveness make it a common practice in other areas[4]. For these reasons, MG must be detected in order to minimize human health risks and water contamination.

Multiple techniques have been developed for detecting MG, such as high-performance liquid chromatography with visible detection (HPLC-VIS)[5], liquid chromatography–mass spectrometry (LC-MS)[6], spectrophotometry[7], enzyme-linked immune sorbent assays (ELISA)[8], capillary electrophoresis–Raman spectroscopy (CE-RS)[9], and surface-enhanced Raman scattering (SERS)[10]. SERS is a technique that amplifies the Raman signal from molecules adsorbed onto nanostructured or roughened metal surfaces. This technology is widely used because it enables the rapid analysis of samples and the identification of molecular fingerprints in real-time, with high sensitivity, and without damaging the sample[11].

Cite this article : Tran N H T, Hoang B K, N T T P, Nguyen D Q N, Nguyen B T, Le H T, Tran T V, H V L, Hoang D V. **Synergistic Au/Ag-based SERS platform for sensitive detection of malachite green**. *Sci. Tech. Dev. J.* 2025; 28(3):3817-3822.

Multiple techniques have been developed for detecting malachite green (MG) in the literature, such as high performance liquid chromatography with visible detection (HPLC-VIS)[5], liquid chromatography-mass spectrometry (LC-MS)[6], spectrophotometry[7], enzyme-linked immune sorbent assay (ELISA)[8], capillary electrophoresis-Raman spectroscopy (CE-RS)[9], surface-enhanced Raman scattering (SERS)[10], etc. SERS is a technique that amplifies the Raman signals of molecules adsorbed onto nanostructured or roughened metal surfaces. This technology is used extensively due to its ability to analyze samples and identify molecular fingerprints quickly, in real time, with highsensitivity, and without damaging the sample[11]. Noble metal nanoparticles, particularly gold (Au NPs) and silver (Ag NPs), are frequently used to fabricate SERS substrates due to their unique optical characteristics. This is attributed to localized surface plasmon resonance (LSPR), an effect in which the free electrons in the metallic nanostructures oscillate collectively, enhancing the optical properties[12]. While both Au and Ag NPs can provide enhancement, Ag NPs generally exhibit stronger plasmonic resonances than Au NPs, often resulting in higher overall signal intensities[13]. The structure of noble metal nanomaterials plays a crucial role in determining the enhancement effect of SERS[14]. The limited functionality of monolayer nanostructures, which often lack the ability to exhibit multiple properties concurrently, significantly restricts their potential applications[15]. Multilayer nanostructures have recently become a focus of significant research due to their potential flexibility in material design. By carefully controlling the plasmon coupling between the various layers, researchers can precisely engineer the intensity and distribution of "hot spots" within these structures, leading to tailored functionalities and enhanced performance[16].

In this work, Au NPs and Ag NPs were deposited on paper (P) substrates to fabricate P/Au monolayers and P/Au/Ag multilayers for sensitive detection of MG using SERS. Notably, the P/Au/Ag substrate demonstrated superior performance, achieving a detection limit as low as 10^{-9} M. These findings highlight the potential applications of the P/Au/Ag substrate in various fields, including environmental monitoring and food safety, where the detection of trace-level contaminants is crucial.

MATERIALS AND METHODS

Materials and reagents

Significant reagents used in this study include gold (III) chloride hydrate ($HAuCl_4.3H_2O$, 99%), sodium citrate (Na_3Ctr, 99%), silver nitrate ($AgNO_3$, 98%), hydrogen peroxide (H_2O_2 solution 30%), sodium borohydride ($NaBH_4$, 98%), and malachite green ($C_{23}H_{25}ClN_2$, 99%) which were all purchased from Sigma Aldrich, USA. Microfiber filter paper (0.26 mm thick, 47 mm diameter, 1.6 μm pore size) was supplied by Whatman, UK. All materials were analytical-grade and were used without further purification.

Preparation of gold nanoparticles (Au NPs) and silver nanoparticles (Ag NPs)

In this study, we propose two different procedures to synthesize Au NPs and Ag NPs solution, as depicted in Figure 1.

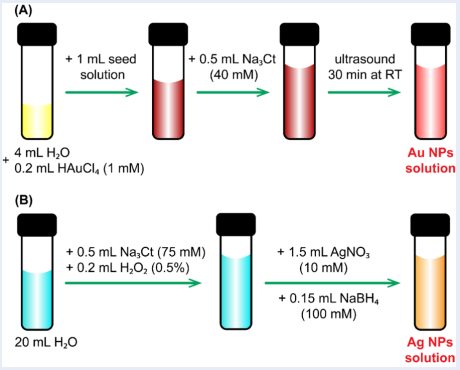

Figure 1: Vital steps in material synthesis of: (A) Au NPs; (B) Ag NPs

Using the seed solution from our previous work[17], Au NPs were prepared with different amounts of reagents to obtain the optimized nanostructures. First, 4 mL of deionized water (DI) was mixed with 0.2 mL of $HAuCl_4$ (1 mM) by vigorous shaking to form a yellow solution. Then, 1 mL of the seed solution and 0.5 mL Na_3Ct (40 mM) were added, and the mixture was placed in an ultrasonic bath for 30 minutes at room temperature. The final Au NP solution was pink (Figure 1A).

Figure 1B shows the fabrication process of Ag NPs. First, 0.5 mL of Na_3Ct (75 mM) and 0.2 mL of H_2O_2 (0.5%) were added to 20 mL of DI water. Then, 1.5 mL of $AgNO_3$ (10 mM) was added to the mixture. Finally, 0.15 mL $NaBH_4$ (100 mM) was added dropwise, which turned the clear solution yellow-orange. The resulting Ag NP and Au NP solutions were stored in cool conditions (4–10°C), avoiding direct light.

Paper modification of Au NPs and Ag NPs

In this study, the SERS signals of MG from Au NPs monolayers were compared with those of Ag/Au double layers. For the P/Au monolayers, 20 μL of Au NP

solution was dropped onto paper substrates, which were allowed to dry unassisted at room temperature. Likewise, for the P/Au/Ag substrate, 20 μL of Ag NP solution was dropped onto the previously prepared P/Au monolayers and allowed to dry without any modifications. Then, 20 μL of MG solutions of various concentrations was added to the SERS substrates. Using a MIRA XTR portable Raman spectrometer with a 785 nm laser, the SERS signals were collected. The enhancement abilities of the P/Au and P/Au/Ag SERS substrates were compared.

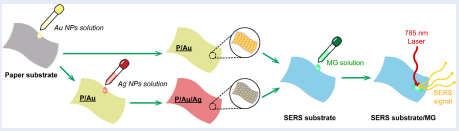

Figure 2: Preparation steps for portable Raman measurements

Analytical Methods

The crystallinity was evaluated using a D8 Advance diffractometer (Bruker, UK) with a Cu X-ray source. The optical and structural properties were determined with a V-730 UV-Vis spectrophotometer (JASCO, Japan). Field-emission scanning electron microscopy (FE-SEM) (Hitachi S-4800, Japan) in conjunction with energy-dispersive X-ray spectroscopy (EDS) was used to examine the shape and composition of the nanostructures. A handheld Robot-Mounted Raman spectrometer (MIRA XTR, Metrohm, Switzerland) with a 785 nm laser at $\leq$ 100 mW was used for the Raman measurements.

RESULTS

The optical properties of well-dispersed Au and Ag NP solutions, characterized by pink and yellow-orange colors, respectively, were investigated using UV-Vis absorption spectroscopy. UV-Vis absorption spectra were acquired for the samples over the range 350–800 nm. Figure 3A presents the absorption spectra, revealing pronounced plasmon resonance features. Au NPs peak at 407 nm, and Ag NPs peak at 526 nm. Figure 3B shows the X-ray diffraction patterns obtained for the Au and Ag NPs. The gold and silver nanoparticles exhibited a characteristic diffraction peak at 2θ=38.2°, indicative of the (111) lattice plane (JCPDS 4-0783 and 4-0784).

The morphologies and sizes of the synthesized Au and Ag NPs were investigated using FE-SEM, as shown in Figure 4. FE-SEM images (Figure 4A and Figure 4B)

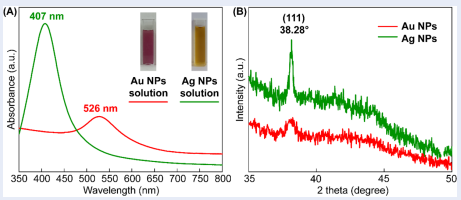

Figure 3: UV-vis spectrum (A) and XRD pattern (B) of Au and Ag NPs solution

show that the synthesized Au and Ag NPs are spherical, with mean diameters of 28.88 and 20.35 nm, respectively (Figure 4C and D). The EDS spectrum of the P/Au/Ag substrate (Figure 4E) shows key peaks corresponding to Au and Ag.

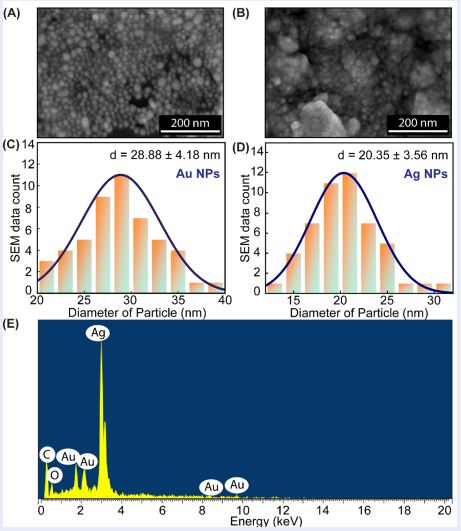

Figure 4: FE-SEM image of (A) Au NPs, (B) Ag NPs; Size distribution histogram of(C) Au NPs and (D) Ag NPs; (E) EDS spectrum of P/Au/Ag

Figure 5A presents the results of the experiments designed to test the enhancement ability of P/Au/MG and P/Au/Ag/MG substrates using a 10^{-3} M solution of MG. The SERS spectrum of MG exhibits several prominent and characteristic vibrational bands. Notably, strong signals are observed at 1175 (C-H bending), 1372 (C-H stretching), 1403 (N-C stretching), and 1620 (N-C, C-C stretching) cm^{-1}. These peaks form a distinctive spectroscopic fingerprint, which, as detailed in Table **??**, allows for the accurate and sensitive detection of MG on our developed SERS platform.

Figure 5B compares the Raman enhancement capabilities of the P/Au/MG and P/Au/Ag/MG substrates

Table 1: Vibrational mode assignments for MG

Wavenumbers (cm^{-1})	Assignment	Reference	Wavenuml (cm^{-1})	Assignment
1175	C-H (bending)	18	1449	$-CH_3$ (bending)
1222	C-H (rocking)	19	1489	$-CH_3$ (bending)
1299, 1372	C-H (bending) and C-C (stretching)	18,20	1595	C-C (stretching)
1403	N-C (stretching)	19	1620	N-C, C-C (stretching)

at 1175, 1372, 1403 and 1620 cm^{-1} at an MG concentration of 10^{-3} M. Figure 5C shows the SERS spectra of MG solutions with concentrations ranging from 10^{-3} to 10^{-9} M using P/Au/Ag as the substrate. The lowest detectable concentration was 10^{-9} M; characteristic peaks were distinguishable at 1372 and 1620 cm^{-1}. The signal at 1620 cm^{-1} in the SERS spectra was used to plot a standard curve relating the Raman peak intensity to the MG concentration (Figure 5D). By taking the logarithm of the MG concentration and fitting it linearly to the corresponding peak intensities, the equation y = −404x + 4202 was obtained, where y represents the peak height at 1620 cm^{-1} and x is the logarithm of the MG concentration. The reliability value (R2) is remarkably high, 0.974.

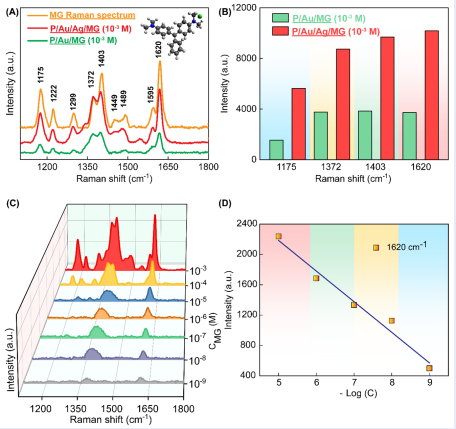

Figure 5: (A) MG Raman spectrum and Raman spectra of P/Au/MG and P/Au/Ag/MG atconcentration of 10^{-3} M, (B) Comparison of peak intensities atwavenumbers 1175, 1372, 1403, 1620 cm^{-1} of P/Au/MG and P/Au/Ag/MG atconcentration of 10^{-3} M, (C) SERS spectra of MG on P/Au/Ag substratewith concentrations from 10^{-3} – 10^{-9} M and (D) Standardcurve calibrated between −log C (MG concentration) and peak intensities at 1620 cm^{-1}

DISCUSSION

The LSPR peak at 526 nm and the pink color of the solution confirm the successful synthesis of spherical Au NPs, a morphology chosen for their suitability in bioapplications[18]. The surface plasmon resonance of the Ag NPs was observed at 407 nm using UV-Vis spectroscopy, confirming the successful synthesis of the Ag NPs[19]. Furthermore, XRD analysis revealed a prominent peak at 2θ = 38.2°, consistent with the (111) lattice plane, which confirms the face-centered cubic (FCC) structure of the Au and Ag NPs[20]. These findings confirm the successful synthesis of spherical Au and Ag NPs, demonstrating their viability for application in SERS-based analytical techniques.

FE-SEM observations confirmed the morphological, dimensional, and structural properties of the synthesized Au and Ag NPs, notably their spherical shape and characteristic average diameter. FE-SEM images indicate that the majority of the Au or Ag NPs have a spherical morphology, with mean diameters of roughly 29 and 20 nm, respectively. Nonetheless, some discernible aggregation occurs, likely stemming from the elevated surface energy characteristic of these particles[21]. Despite this tendency to cluster, the size distribution remains reasonably uniform, suggesting that the synthesis procedure was largely well-managed. The EDS spectrum also demonstrated the significant presence of MG on the P/Au/Ag structure with increasing intensity of key peaks. Additional peaks from C and O appeared due to the paper substrate.

In a set of comparative SERS measurements for MG at a concentration of 10^{-3} M, two distinct substrates were investigated: P/Au/MG and P/Au/Ag/MG. Initial observations showed that adding an Ag layer to the P/Au substrate (forming a P/Au/Ag/MG substrate) led to increases in the Raman signals, such that the intensities of the malachite green peaks surpassed those of the P/Au/MG substrate. This can be ascribed to the synergistic effects of arranging the Au and Ag layers in a multilayer configuration. Thanks to these multilayers, the LSPR phenomena from each metal layer overlap, creating an elevated density of hot spots on the substrate. These hot spots intensify the electromagnetic field around the adsorbed MG molecules, amplifying the Raman signal beyond that of a single metal layer[22,23]. Consequently, the P/Au/Ag/MG substrate demonstrates a more efficient and robust SERS response, highlighting the advantages of a multilayer Au/Ag design for high-sensitivity molecular detection.

In analyzing the SERS spectra of MG on a P/Au/Ag substrate, distinct vibrational peaks were detectable down to a concentration of 10^{-9} M. The specific SERS signal for MG and the R2 value are indisputable evidence of the signal enhancement ability of the P/Au/Ag substrate. As a result, the P/Au/Ag substrate holds considerable promise for trace-level detection as required in applications such as water quality monitoring and food safety in aquaculture. The robust and reproducible feature of this multilayer structure further positions it as a powerful platform for the rapid identification of other low-concentration contaminants in complex environments.

CONCLUSIONS

In this study, a P/Au/Ag substrate for the SERS-based detection of MG was successfully fabricated, achieving sensitivity down to 10^{-9} M. Comprehensive characterization by UV-Vis, XRD, HR-TEM, and FE-SEM confirmed the formation of a robust multilayer structure, in which the synergy between gold and silver significantly enhanced the SERS signal. These results emphasize that the substrate is not only highly effective for detecting MG at trace levels but also holds wide-ranging promise for environmental monitoring and food safety applications. Future work will focus on optimizing the substrate architecture and extending its use to detect other critical contaminants.

COMPETING INTERESTS

The author(s) declare that they have no competing interests.

AUTHORS' CONTRIBUTIONS

All the authors read and corrected the submitted final version.

Nguyen Do Quynh Nhu, Le Hong Tho conceived experiments design, analyzed data, carried out, and wrote the manuscript with support from Dr. Nhu Hoa Thi Tran. Nguyen Bao Tran, Nguyen Tran Truc Phuong carried out the experiments in group. Hieu Van Le, Tran T.T. Van, Dung Hoang Van have supported the analysis techniques. Dr. Nhu Hoa Thi Tran revised and corrected the manuscript.

ABBREVIATIONS

Au NPs: gold nanoparticles
Ag NPs: silver nanoparticles
P: paper
FCC: face-centered cubic
MG: malachite green
LSPR: localized surface plasmon resonance
LOD: detection of limited
XRD: X-ray diffraction
EDS: energy dispersive X-ray spectroscopy
FE-SEM: field-emission scanning electron microscopy
HR-TEM: high-resolution transmission electron microscopy
UV-vis: ultraviolet-visible spectroscopy
SERS: surface-enhanced Raman scattering

ACKNOWLEDGEMENTS

This research is funded by Vietnam National Foundation for Science and Technology Development (NAFOSTED) under grant number 103.03-2023.51. We would like to gratefully acknowledge the Center for Innovative Materials and Architectures (Laboratory for Optics and Sensing) at Vietnam National University in Ho Chi Minh City

REFERENCES

1. EZ T, PG Y, TT Y, H W, L G. Three dimensional design of large-scale TiO 2 nanorods scaffold decorated by silver nanoparticles as SERS sensor for ultrasensitive malachite green detection. ACS Appl Mater Interfaces. 2012;4(7):3432–3437.
2. J S, S S, V S. Toxicity of malachite green on plants and its phytoremediation: A review. Regional Studies in Marine Science Elsevier. 2023;62:102911.
3. P K, R K, M S, D D, SK S. A highly sensitive, flexible SERS sensor for malachite green detection based on Ag decorated microstructured PDMS substrate fabricated from Taro leaf as template. Sensors Actuators, B Chem. 2016;246:477–486.
4. X Z, J Z, and Li D PZ. Review of Methods for the Detection and Determination of Malachite Green and Leuco-Malachite Green in Aquaculture. Critical Reviews in Analytical Chemistry Taylor & Francis. 2019;49:1–20.
5. J X, T P, DD C, QJ Z, GM W, X W, et al. Determination of malachite green, crystal violet and their leuco-metabolites in fish by HPLC-VIS detection after immunoaffinity column clean-up. J Chromatogr B Anal Technol Biomed Life Sci. 2013;913-914:123–128.

6. MJ MB, S H, A U, A A, MD H, et al. Determination of malachite green residues in fish using molecularly imprinted solid-phase extraction followed by liquid chromatography-linear ion trap mass spectrometry. Anal Chim Acta. 2010;665(1):47–54.
7. R M, M B. Simultaneous preconcentration and determination of malachite green and fuchsine dyes in seafood and environmental water samples using nano-alumina-based molecular imprinted polymer solid-phase extraction. Int J Environ Anal Chem. 2016;96(6):576–594.
8. N B, and Kolanović BS VI, D O, S Z. Malachite green residues in farmed fish in Croatia. Food Control. 2012;26(2):393–396.
9. CH T, Der LJ, CH L. Optimization of the separation of malachite green in water by capillary electrophoresis Raman spectroscopy (CE-RS) based on the stacking and sweeping modes. Talanta. 2007;72(2):368–372.
10. ning LY, jun LJ, jun WG, J Z, wu ZJ. Reliable detection of malachite green by self-assembled SERS substrates based on gold–silicon heterogeneous nano pineapple structures. Food Chem. 2024;451:139454.
11. ZH L, JH B, X Z, JM L, CS F, YM Z, et al. Facile synthesis of Au nanoparticle-coated Fe3O4 magnetic composite nanospheres and their application in SERS detection of malachite green. Spectrochim Acta - Part A Mol Biomol Spectrosc. 2020;241:118532.
12. J B, P K, S T, D K, S P. Plasmonic nanoparticles and their analytical applications: A review. Applied Spectroscopy Reviews Taylor & Francis. 2017;52:774–820.
13. PK J, X H, IH ES, MA ES. Noble metals on the nanoscale: Optical and photothermal properties and some applications in imaging, sensing, biology, and medicine. Acc Chem Res. 2008;41(12):1578–1586.
14. X Z, H Z, L Y, N L, J S, C J. Recent Developments in Detection Using Noble Metal Nanoparticles. Critical Reviews in Analytical Chemistry Taylor & Francis. 2020;50:97–110.
15. Q G, J Z, jun WG, jun LJ, wu ZJ. Core-satellite nanostructures and their biomedical applications. Microchimica Acta Mikrochim Acta. 2022;189.
16. X W, C H, J K, H K, NA K, LM LM, et al. Environmentally responsive plasmonic nanoassemblies for biosensing: Chemical Society Reviews. The Royal Society of Chemistry. 2018;4677(4696).
17. PQT D, VT H, NTT P, TH N, HKT T, H J, et al. The highly sensitive determination of serotonin by using gold nanoparticles (Au NPs) with a localized surface plasmon resonance (LSPR) absorption wavelength in the visible region. RSC Adv. 2020;10(51):30858–30869.
18. PN N, IIS L, D M, HY P, B K, S M, et al. Size correlation of optical and spectroscopic properties for gold nanoparticles. J Phys Chem C. 2007;111(40):14664–14669.
19. CW L, AP C, TT L, JH L. Antimicrobial activity of UV-induced chitosan capped silver nanoparticles. Mater Lett. 2014;128:248–252.
20. S Y, J M, BL D. Phytosynthesis of stable Au, Ag and Au-Ag alloy nanoparticles using J. Sambac leaves extract, and their enhanced antimicrobial activity in presence of organic antimicrobials. Spectrochim Acta - Part A Mol Biomol Spectrosc. 2015;137(1):236–243.
21. QH T, VQ N, AT L. Silver nanoparticles: Synthesis, properties, toxicology, applications and perspectives. Advances in Natural Sciences: Nanoscience and Nanotechnology IOP Publishing. 2013;4:033001.
22. Y W, B Y, L C. SERS Tags: Novel optical nanoprobes for bioanalysis. Chemical Reviews American Chemical Society. 2013;113:1391–1428.
23. B S, RR F, Al H, E R, Van Duyne RP. SERS: Materials, applications, and the future. Materials Today Elsevier. 2012;15:16–25.